IOPscience iopscience.iop.org

Home Search Collections Journals About Contact us My IOPscience

Luminescence and optical absorption properties of $Nd^{3+}$ ions in K–Mg–Al phosphate and fluorophosphate glasses

This article has been downloaded from IOPscience. Please scroll down to see the full text article.

2006 J. Phys.: Condens. Matter 18 3975

(http://iopscience.iop.org/0953-8984/18/16/007)

View the table of contents for this issue, or go to the journal homepage for more

Download details:
IP Address: 129.252.86.83
The article was downloaded on 28/05/2010 at 10:09

Please note that terms and conditions apply.

INSTITUTE OF PHYSICS PUBLISHING JOURNAL OF PHYSICS: CONDENSED MATTER

J. Phys.: Condens. Matter **18** (2006) 3975–3991 doi:10.1088/0953-8984/18/16/007

# Luminescence and optical absorption properties of $Nd^{3+}$ ions in K–Mg–Al phosphate and fluorophosphate glasses

**S Surendra Babu[1], P Babu[2], C K Jayasankar[1,5], A S Joshi[3], A Speghini[4] and M Bettinelli[4]**

[1] Department of Physics, Sri Venkateswara University, Tirupati-517 502, India
[2] Department of Physics, Government Degree College, Wanaparthy-509 103, India
[3] High Power Laser Optics Laboratory, Laser Plasma Division, Centre for Advanced Technology, Indore-452 013, India
[4] Dipartimento Scientifico e Tecnologico, Università di Verona and INSTM, UdR Verona, Ca'Vignal, Strada Le Grazie 15, I-37134 Verona, Italy

E-mail: ckjaya@yahoo.com

Received 5 January 2006
Published 7 April 2006
Online at stacks.iop.org/JPhysCM/18/3975

**Abstract**

Absorption and emission properties and fluorescence lifetimes for the $^4F_{3/2} \rightarrow {}^4I_{11/2}$ transition of $Nd^{3+}$ ions embedded in $P_2O_5$–$K_2O$–MgO–$Al_2O_3$ (PKMA)-based glasses modified with $AlF_3$ and $BaF_2$ are reported at room temperature. The observed energy levels of $Nd^{3+}$ ions in these glasses have been analysed through a semi-empirical free-ion Hamiltonian model. The spin–orbit interaction and net electrostatic interaction experienced by the $Nd^{3+}$ ions follow the trend as PKMA > PKMA + $AlF_3$ > PKMA + $BaF_2$ glasses. Judd–Ofelt analysis has been carried out on the absorption spectra of 1.0 mol% $Nd^{3+}$-doped glasses to predict the radiative properties for the fluorescent levels of the $Nd^{3+}$ ion. Branching ratios and stimulated emission cross-sections show that the $^4F_{3/2} \rightarrow {}^4I_{11/2}$ transition of the glasses under investigation has the potential for laser applications. The Inokuti–Hirayama model has been applied to investigate the non-radiative relaxation of the $Nd^{3+}$ ion emitting state, $^4F_{3/2}$. Based on the decay curve analysis, concentration quenching of the $^4F_{3/2}$ emission has been attributed to a cross-relaxation process between the $Nd^{3+}$ ions.

## 1. Introduction

$Nd^{3+}$-doped glasses have been extensively investigated to assess the laser properties for the design of glass laser systems. Among the $^4F_{3/2} \rightarrow {}^4I_J$ ($J = 9/2, 11/2, 13/2$ and $15/2$) emission transitions of the $Nd^{3+}$ ion, the $^4F_{3/2} \rightarrow {}^4I_{11/2}$ transition in the vicinity of 1.06 $\mu$m is

[5] Author to whom any correspondence should be addressed.

 © 2006 IOP Publishing Ltd Printed in the UK 

of interest for research as well as for industrial lasers because of its efficient pumping by flash lamps and other lasers and its ease of operation at room temperature. The other lasing transition $^4F_{3/2} \rightarrow {}^4I_{9/2}$ at around 0.88 $\mu$m is finding application as a powerful diode laser. On the other hand, the $^4F_{3/2} \rightarrow {}^4I_{13/2}$ transition of the $Nd^{3+}$ ion is serving as a 1.3 $\mu$m telecommunications transition window. As the physical and optical properties of these $Nd^{3+}$-doped glasses depend on the host glass matrix, a great amount of research has been undertaken with the aim of finding glasses with better optical performance and high quantum efficiency [1].

Among the variety of laser glass hosts investigated for the $Nd^{3+}$ ion, metaphosphate-based glasses were found to be efficient hosts, especially for high-energy and high-peak-power laser outputs up to multi-kilojoules and multi-terawatts. These glass lasers are useful for fusion energy research because they have excellent energy storage capability and extraction characteristics and can be made in large sizes with high optical quality, free of damage-causing inclusions [2]. Typically, phosphate glasses exhibit good chemical durability, relatively large thermal expansion coefficient and low optical dispersion [3]. The main disadvantages of phosphate glasses for their use as laser hosts are their larger thermal expansion and lower fracture toughness than silicate glasses [4]. Even though these glasses have such disadvantages, they are preferred as laser hosts because they possess low refractive index, low melting temperature, good thermo-optical performance and low glass transition temperature [5, 6].

Detailed spectroscopic properties of $P_2O_5$–$K_2O$–$Al_2O_3$ (PKA) glass modified with BaO, BaO/$BaF_2$ and BaO/$AlF_3$ have been presented in our earlier paper [7]. In the present investigation the optical properties of $Nd^{3+}$-doped PKA-based glass modified with MgO, MgO/$BaF_2$ and MgO/$AlF_3$ are studied through measurements of their optical absorption and luminescence spectra and emission decay curves. The electronic structure of $Nd^{3+}$ ions in these glasses is deduced by means of a free-ion Hamiltonian model. The Judd–Ofelt parameters are calculated and are in turn used to evaluate transition probabilities, radiative lifetimes, branching ratios and peak stimulated emission cross-sections for the luminescent levels. All these predicted radiative properties are found to be in agreement with those obtained experimentally. The peak stimulated emission cross-section for the $^4F_{3/2} \rightarrow {}^4I_{11/2}$ transition of the $Nd^{3+}$ ion is found to be $4.46 \times 10^{-20}$ cm$^2$ for the PKA glass modified with MgO/$BaF_2$, which is higher than those obtained for other $Nd^{3+}$-doped glasses. A careful analysis of the emission decay curves has been performed to unravel the nature of non-radiative processes which limit the radiative properties in these glasses.

## 2. Experimental details

Table 1(a) presents the compositions (in mol%) of the glass samples used in the present work. To prepare these samples, reagent-grade $Al(PO_3)_3$, $Mg(PO_3)_2$, $KH_2PO_4$ and $Nd_2O_3$ were mixed and crushed thoroughly in an agate mortar and the homogeneous mixtures were fired in an electronic furnace at a temperature of 1075 °C for 45 min. The melts were then poured on a preheated brass mould and annealed at 350 °C for about 5 h to remove thermal strains. Thus glass samples with good optical quality were obtained. They were also found to be stable against atmospheric moisture. Then the glass samples were allowed to cool to room temperature (RT) and were polished for optical measurements. The refractive index, $n$, was measured on an Abbe refractometer at sodium wavelength (589.3 nm). The density was measured by the Archimedes method using water as an immersion liquid. Various physical properties such as refractive index, density, concentration and optical path length of the 1.0 mol% $Nd^{3+}$-doped title glasses are presented in table 1(b).

The absorption spectra were measured on a spectrophotometer (Hitachi U-3400) in the 325–950 nm wavelength range. The NIR emission spectra (800–1600 nm) were recorded using

**Table 1.** (a) Glass compositions and glass labels of the $Nd^{3+}$-doped PKMA-based glasses. (b) Physical properties, nephelauxetic ratios and bonding parameters of 1.0 mol% $Nd^{3+}$-doped PKMA-based glasses.

| (a) Glass composition | Label |
|---|---|
| 58.95 $P_2O_5$ + 17.45 $K_2O$ + 14.5 MgO + 9.0 $Al_2O_3$ + 0.1 $Nd_2O_3$ | PKMAN01 |
| 58.5 $P_2O_5$ + 17.0 $K_2O$ + 14.5 MgO + 9.0 $Al_2O_3$ + 1.0 $Nd_2O_3$ | PKMAN10 |
| 58.0 $P_2O_5$ + 17.0 $K_2O$ + 14.0 MgO + 9.0 $Al_2O_3$ + 2.0 $Nd_2O_3$ | PKMAN20 |
| 55.95 $P_2O_5$ + 17 $K_2O$ + 11.95 MgO + 9 $Al_2O_3$ + 6 $BaF_2$ + 0.1 $Nd_2O_3$ | PKMABFN01 |
| 55.5 $P_2O_5$ + 17 $K_2O$ + 11.5 MgO + 9 $Al_2O_3$ + 6 $BaF_2$ + 1.0 $Nd_2O_3$ | PKMABFN10 |
| 55 $P_2O_5$ + 17 $K_2O$ + 11 MgO + 9 $Al_2O_3$ + 6 $BaF_2$ + 2.0 $Nd_2O_3$ | PKMABFN20 |
| 56.6 $P_2O_5$ + 16.75 $K_2O$ + 14.73 MgO + 8.37 $Al_2O_3$ + 3.45 $AlF_3$ + 0.1 $Nd_2O_3$ | PKMAFN01 |
| 56.15 $P_2O_5$ + 16.75 $K_2O$ + 14.28 MgO + 8.37 $Al_2O_3$ + 3.45 $AlF_3$ + 1.0 $Nd_2O_3$ | PKMAFN10 |
| 55.65 $P_2O_5$ + 16.75 $K_2O$ + 13.78 MgO + 8.37 $Al_2O_3$ + 3.45 $AlF_3$ + 2.0 $Nd_2O_3$ | PKMAFN20 |

| (b) Properties | PKMAN10 | PKMABFN10 | PKMAFN10 |
|---|---|---|---|
| Refractive index, $n$ | 1.528 | 1.534 | 1.530 |
| Density, $d$ (g $ml^{-1}$) | 2.487 | 2.541 | 2.564 |
| Concentration, $C$ ($10^{20}$ ions $cm^{-3}$) | 2.425 | 2.380 | 2.539 |
| Optical path length (cm) | 0.357 | 0.358 | 0.370 |
| Nephelauxetic average ratio ($\bar{\beta}$) | 1.2394 | 1.2349 | 1.2395 |
| Bonding parameter ($\delta$) | −19.318 | −19.022 | −19.338 |

a Jarrell–Ash $\frac{3}{4}$ m Czerny–Turner single monochromator. The signal was detected by a liquid nitrogen-cooled Northcoast EO-817P germanium detector connected to a computer-controlled Stanford Research SR510 lock-in amplifier. The emission decay curves were measured by exciting the samples with the third harmonic radiation ($\lambda_{exc}$ = 355 nm) of a pulsed Nd–YAG laser. The signal was then analysed using a 0.5 m monochromator equipped with a 150 lines $mm^{-1}$ grating and detected with a GaAs PMT and a digital oscilloscope.

## 3. Theoretical background

The model free-ion Hamiltonian ($H_{FI}$) that was used to study the electronic energy level structure of $Nd^{3+}$ ions and the fitting procedure for the observed and calculated energy level scheme were similar to those reported in [7–9]. The theory of the Judd–Ofelt (JO) analysis has been well described elsewhere [10, 11]. Following the same procedure as reported in [7–13], the JO parameters and in turn the radiative and non-radiative properties for the fluorescent levels of $Nd^{3+}$ ions in the present glasses have been estimated.

## 4. Results

The optical absorption spectra for 1.0 mol% $Nd^{3+}$-doped PKMAN10, PKMAFN10 and PKMABFN10 glasses, measured in the 325–950 nm spectral region at RT, are shown in figure 1. The assignments of the absorption bands originating from the ground $^4I_{9/2}$ state to various excited states within the 4f shell are also shown in the figure 1. These bands were identified by comparison with $Nd^{3+}$ ion in the aquo-ion system [14] and $Nd^{3+}$:glass systems [5, 8, 9, 15–32]. These spectra are very similar to those found for other $Nd^{3+}$-doped glass systems [5, 8, 9, 15–32], except for some small changes in the band positions and relative intensities. The absorption band positions for the 1.0 mol% $Nd^{3+}$-doped PKMAN10, PKMAFN10 and PKMABFN10 glasses occur at almost the same wavenumbers and are presented in table 2. The nephelauxetic ratios and bonding parameters [7–9]

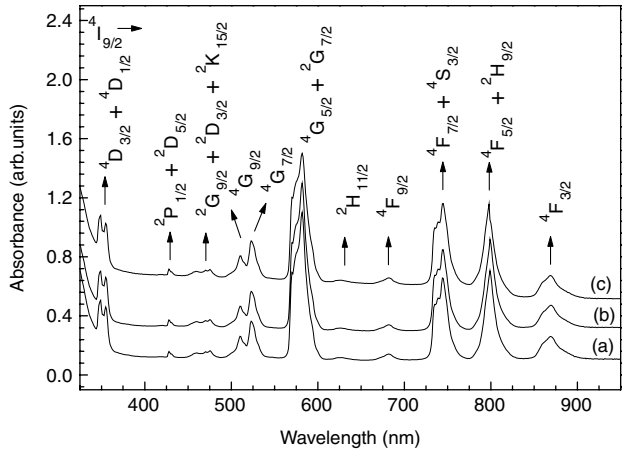


**Figure 1.** Optical absorption spectra of 1.0 mol% $Nd^{3+}$-doped (a) PKMAN10, (b) PKMAFN10 and (c) PKMABFN10 glasses.

obtained from these energy level data are presented in table 1(b). The experimental absorption band positions for some reported $Nd^{3+}$-doped glass systems which include $P_2O_5$–$K_2O$–BaO–$Nd_2O_3$ (PKBN) [18], CaO–$SiO_2$–$P_2O_5$–$Nd_2O_3$ (CSPN) [19], $TeO_2$–LiF–$Nd_2O_3$ (TLN) [25], $BaF_2$–$InF_3$–$GaF_3$–$ZnF_2$–$LnF_3$–$ThF_4$–$MnF_2$–$NdF_3$ (BIGZLTM) [30], $NaPO_3$–$CaF_2$–$NdF_3$ (NCN) [31] and ZnO–$B_2O_3$–$Nd_2O_3$ (ZBN) [32] are also shown in table 2. The best-fit set of free-ion parameters obtained by minimizing the rms deviation between the experimental and calculated energy levels is presented in table 3. The calculated energy levels obtained using the best-fit free-ion parameters are also presented in table 2 for the present glass systems.

The experimental oscillator strengths of various observed transitions are evaluated from the absorption spectra [21]. A least-squares fitting approach is then adopted between the experimental and calculated oscillator strengths to determine the JO parameters. The experimental ($f_{exp}$) and theoretical ($f_{cal}$) oscillator strengths obtained from JO theory are presented in table 4 together with the experimental oscillator strengths for some of the reported $Nd^{3+}$:glass systems that include PKBN [18], CSPN [19], TLN [25] and ZBN [32]. Table 5 presents the $\langle \|U^{(\lambda)}\| \rangle^2$ values for PKMAN10 glass which are determined through the intermediate coupling approximation by generating the wavefunctions using the free-ion parameters given in table 3 for the $Nd^{3+}$:PKMAN10 glass. Neglecting higher multipolar interactions such as the electric quadrupole, etc, the total oscillator strength $f_{total}$ of a band is given by the sum of electric and magnetic dipole oscillator strengths [33] as

$$f_{total} = f_{ed} + f_{md} \tag{1}$$

where

$$f_{ed} = \frac{8\pi^2 mc\nu}{3he^2(2J+1)} \frac{(n^2+2)}{9n} S_{ed} \tag{2}$$

and

$$f_{md} = \frac{8\pi^2 mc\nu}{3he^2(2J+1)} n S_{md} \tag{3}$$

where $S_{ed}$ and $S_{md}$ are the electric and magnetic dipole line strengths, respectively. The values of $f_{ed}$, $f_{md}$ and $f_{total}$ for $Nd^{3+}$:PKMAN10 glass are also presented in table 5.

**Table 2.** Wavenumbers (in $cm^{-1}$) of experimental and calculated peak positions of absorption bands for 1.0 mol% $Nd^{3+}$-doped glasses under investigation and experimental peak positions for some reported $Nd^{3+}$:glass systems.

| | PKMAN10 | | PKMAFN10 | | PKMABFN10 | | PKBN [18] | CSPN [19] | TLN [25] | BIGZLTM [30] | NCN [31] | ZBN [32] |
|---|---|---|---|---|---|---|---|---|---|---|---|---|
| Transition $^4I_{9/2} \rightarrow$ | $E_{exp}$ | $E_{cal}$ | $E_{exp}$ | $E_{cal}$ | $E_{exp}$ | $E_{cal}$ | $E_{exp}$ | $E_{exp}$ | $E_{exp}$ | $E_{exp}$ | $E_{exp}$ | $E_{exp}$ |
| $^4I_{9/2}$ | 0 | −33 | 0 | −20 | 0 | −18 | 0 | 0 | 0 | 0 | 0 | 0 |
| $^4I_{11/2}$ | 1 659 | 1 771 | 1 710 | 1 794 | 1 720 | 1 796 | 1 718 | 1 947 | — | — | — | — |
| $^4I_{13/2}$ | 3 591 | 3 703 | 3 650 | 3 736 | 36 640 | 3 737 | 3 608 | 4 082 | — | 4 028 | — | — |
| $^4I_{15/2}$ | — | 5 725 | — | 5 765 | — | 5 766 | — | 6 135 | — | 6 099 | — | — |
| $^4F_{3/2}$ | 11 507 | 11 411 | 11 507 | 11 416 | 11 507 | 11 420 | 11 468 | 11 363 | 11 409 | 11 541 | 11 578 | 11 417 |
| $^4F_{5/2}$ | — | 12 414 | — | 12 426 | — | 12 429 | 12 484 | 12 438 | 12 422 | 12 539 | 12 486 | 12 465 |
| $^2H(2)_{9/2}$ | 12 516 | 12 678 | 12 516 | 12 677 | 12 531 | 12 668 | — | — | — | — | — | — |
| $^4F_{7/2}$ | 13 411 | 13 371 | 13 423 | 13 386 | 13 423 | 13 389 | — | 13 387 | 13 351 | 13 492 | 13 406 | 13 439 |
| $^4S_{3/2}$ | 13 605 | 13 455 | 13 605 | 13 469 | 13 605 | 13 473 | 13 405 | — | — | — | — | — |
| $^4F_{9/2}$ | 14 620 | 14 619 | 14 620 | 14 638 | 14 641 | 14 638 | 14 620 | 14 641 | 14 609 | 14 730 | 14 636 | 14 686 |
| $^2H_{11/2}$ | 16 000 | 15 916 | 15 974 | 15 929 | 15 924 | 15 917 | — | 15 873 | 16 000 | 15 952 | 15 863 | 15 921 |
| $^4G_{5/2}$ | 17 182 | 17 217 | 17 182 | 17 217 | 17 182 | 17 222 | 17 182 | 17 123 | 17 079 | — | 17 209 | 17 186 |
| $^2G_{7/2}$ | 17 513 | 17 358 | 17 544 | 17 361 | 17 544 | 17 355 | — | — | — | 17 346 | — | — |
| $^4G_{7/2}$ | 19 120 | 19 092 | 19 120 | 19 101 | 19 120 | 19 098 | 19 084 | — | 18 957 | — | 19 033 | 19 220 |
| $^4G_{9/2}$ | — | 19 448 | — | 19 462 | — | 19 462 | — | — | 19 417 | 19 391 | — | — |
| $^2K_{13/2}$ | 19 608 | 19 678 | 19 608 | 19 675 | 19 569 | 19 665 | — | — | — | — | — | — |
| $^2G_{9/2}$ | 21 008 | 21 057 | 21 053 | 21 078 | 21 053 | 21 068 | 21 008 | — | — | — | — | — |
| $^2D_{3/2}$ | 21 277 | 21 216 | 21 277 | 21 206 | 21 277 | 21 203 | — | — | 21 119 | — | 21 255 | 21 366 |
| $^4G_{11/2}$ | — | 21 399 | — | 21 419 | — | 21 422 | — | 21 322 | — | — | — | — |
| $^2K_{15/2}$ | 21 739 | 21 615 | 21 739 | 21 620 | 21739 | 21 610 | — | — | 21 668 | 21 580 | — | — |
| $^2P_{1/2}$ | 23 202 | 23 249 | 23 202 | 23 244 | 23 202 | 23 239 | 23 364 | 23 148 | 23 202 | 23 343 | 23 333 | 23 210 |
| $^2D_{5/2}$ | 23 809 | 23 874 | 23 810 | 23 876 | 23 810 | 23 866 | — | — | — | — | — | — |
| $^2P_{3/2}$ | — | 26 048 | — | 26 057 | — | 26 053 | — | — | — | — | — | — |
| $^4D_{3/2}$ | 28 169 | 28 243 | 28 169 | 28 234 | 28 169 | 28 239 | 28 169 | 28 169 | — | — | — | 28 216 |
| $^4D_{5/2}$ | — | 28 383 | — | 28 371 | — | 28 376 | — | — | — | — | — | — |
| $^4D_{1/2}$ | 28 653 | 28 720 | 28 653 | 28 718 | 28 571 | 28 725 | — | — | — | — | 28 543 | — |
| $\sigma$ $(N)$[a] | ±91 (20) | | ±78 (20) | | ±85 (20) | | ±41 (12) | ±72 (14) | ±37 (12) | ±60 (12) | ±56 (11) | ±72 (11) |

[a] $\sigma$ corresponds to rms deviation and the $N$ value within parentheses represents the number of levels used in the parametric fit. See [7] for details.

**Table 3.** Best-fit free-ion parameters ($cm^{-1}$) for $Nd^{3+}$:glass systems. The values given in parentheses are the uncertainties in the fitted parameters.

| Parameter | PKMAN10 | PKMAFN10 | PKMABFN10 | PKBN [18] | CSPN [19] | TLN [25] | BIGZLTM [30] | NCN [31] | ZBN [32] |
|---|---|---|---|---|---|---|---|---|---|
| $E_{AVG}$ | 24 219(75) | 24 219(70) | 24 217(70) | 24 228(72) | 24 071(77) | 24 148(38) | 24 300(70) | 24 235(61) | 24 129(84) |
| $F^2$ | 72 529(228) | 72 417(214) | 72 438(213) | 72 523(226) | 71 486(236) | 71 808(121) | 72 788(213) | 72 915(199) | 72 051(261) |
| $F^4$ | 54 444(289) | 54 353(271) | 54 248(270) | 55 245(321) | 51 976(287) | 54 115(195) | 51 783(251) | 52 243(336) | 51 576(348) |
| $F^6$ | 35 384(255) | 35 278(239) | 35 246(239) | 36 483(256) | 35 772(269) | 35 446(127) | 35 900(236) | 36 226(210) | 36 514(296) |
| $\zeta$ | 856.2(40) | 860.1(38) | 859.9(37) | 832.2(40) | 897.6(34) | 870.4(25) | 885.0(32) | 857.8(42) | 888.1(44) |
| $\Sigma F^k$ | 162 359 | 162 048 | 161 932 | 164 251 | 159 234 | 161 369 | 160 471 | 161 384 | 160 141 |
| $F^2/F^4$ | 1.332 | 1.332 | 1.335 | 1.313 | 1.375 | 1.327 | 1.405 | 1.397 | 1.397 |
| $F^2/F^6$ | 2.050 | 2.053 | 2.055 | 1.988 | 1.998 | 2.026 | 2.027 | 2.013 | 1.973 |

**Table 4.** Absorption levels (from ground state, $^4I_{9/2}$), experimental ($f_{exp} \pm 5\%$, $\times 10^{-6}$) and calculated ($f_{cal}$, $\times 10^{-6}$) oscillator strengths for 1.0 mol% $Nd^{3+}$-doped title glasses and experimental oscillator strengths for some reported $Nd^{3+}$:glass systems.

| Transition | PKMAN10 | | PKMAFN10 | | PKMABFN10 | | PKBN [18] | CSPN [19] | TLN [25] | ZBN [32] |
|---|---|---|---|---|---|---|---|---|---|---|
| $^4I_{9/2} \rightarrow$ | $f_{exp}$ | $f_{cal}$ | $f_{exp}$ | $f_{cal}$ | $f_{exp}$ | $f_{cal}$ | $f_{exp}$ | $f_{exp}$ | $f_{exp}$ | $f_{exp}$ |
| $^4F_{3/2}$ | 2.93 | 2.98 | 2.87 | 2.69 | 3.05 | 2.99 | 1.82 | 2.06 | 2.82 | 2.00 |
| $^4F_{5/2}$, $^2H_{9/2}$ | 8.73 | 9.31 | 8.63 | 9.15 | 7.90 | 9.25 | 6.76 | 7.51 | 9.64 | 6.90 |
| $^4F_{7/2}$, $^4S_{3/2}$ | 9.88 | 9.58 | 10.01 | 9.74 | 10.33 | 9.43 | 6.63 | 7.29 | 11.99 | 7.62 |
| $^4F_{9/2}$ | 0.83 | 0.74 | 0.80 | 0.74 | 0.94 | 0.73 | 0.75 | 0.50 | 0.76 | 0.60 |
| $^2H_{11/2}$ | 0.16 | 0.21 | 0.29 | 0.21 | 0.40 | 0.20 | — | 0.12 | 0.20 | 0.15 |
| $^4G_{5/2}$, $^2G_{7/2}$ | 25.84 | 25.87 | 28.31 | 28.33 | 28.79 | 28.84 | 15.68 | 19.00 | 31.73 | 21.22 |
| $^4G_{7/2}$ | 5.41 | 4.68 | 4.88 | 4.57 | 5.62 | 4.86 | 4.30[a] | 6.27[a] | 6.00 | 7.20[a] |
| $^4G_{9/2}$ | 4.32 | 2.68 | 4.00 | 2.63 | 4.49 | 2.70 | | | 2.34 | |
| $^2G_{9/2}$, $^2D_{3/2}$, $^2K_{15/2}$ | 2.42 | 1.67 | 2.16 | 1.58 | 2.29 | 1.67 | 4.57[b] | 1.42[b] | 8.21[b] | 1.73[c] |
| $^2P_{1/2}$, $^2D_{5/2}$ | 0.42 | 0.86 | 0.47 | 0.75 | 0.67 | 0.86 | 2.00 | 0.50[d] | 3.43[d] | 0.43[d] |
| $^4D_{3/2}$, $^4D_{1/2}$ | 14.12 | 14.07 | 12.30 | 12.38 | 14.71 | 14.13 | 10.02[e] | 8.67[f] | — | 10.04[g] |
| $\sigma$ ($N$) | ±0.63 (11) | | ±0.50 (11) | | ±0.81 (11) | | ±2.2 (8) | ±0.3 (12) | ±1.69 (11) | ±6.9 (10) |

[a] Includes the oscillator strength (OS) of the $^2K_{13/2}$ level.
[b] Includes the OS of the $^4G_{11/2}$ level.
[c] Includes the combined OS of the $^2P_{3/2}$ and $^4G_{11/2}$ levels.
[d] OS of only the $^2P_{1/2}$ level.
[e] Combined OS of the $^2D_{3/2}$, $^2D_{5/2}$, $^4I_{11/2}$, $^2D_{1/2}$ and $^4I_{15/2}$ levels.
[f] OS of only the $^4D_{5/2}$ and $^2I_{11/2}$ levels; does not include the $^4D_{1/2}$ level.
[g] Includes the OS of the $^4D_{5/2}$, $^4I_{11/2}$ and $^2L_{15/2}$ levels.

Table 6 presents the JO parameters obtained in the present work, and they are compared with those of other reported $Nd^{3+}$-doped glasses. By using these JO parameters along with the refractive index, various radiative properties such as transition probabilities ($A$), lifetimes ($\tau_R$) and branching ratios ($\beta_R$) have been calculated. Table 7 presents these radiative properties for some of the luminescent levels of $Nd^{3+}$:PKMAN10 glass.

The emission spectra of the phosphate glasses under investigation at different $Nd^{3+}$ ion concentration have been recorded in the 6500–12 000 $cm^{-1}$ wavenumber range at RT with an excitation radiation at a wavelength of 355 nm. Figure 2 shows the emission spectra of PKMAN glasses with different $Nd^{3+}$ ion concentration. The emission bands of the spectra correspond to transitions originating from the luminescent $^4F_{3/2}$ level to the $^4I_{13/2}$, $^4I_{11/2}$ and $^4I_{9/2}$ multiplets. The spectra are normalized with respect to the peak intensity of the $^4F_{3/2} \rightarrow {}^4I_{11/2}$ emission transition. The emission spectra of these glasses are similar to each other and are comparable with those obtained for other $Nd^{3+}$-doped glass systems [15, 16, 18–21, 24, 27]. From the emission spectra, the experimental emission peak positions ($\lambda_p$), effective linewidths ($\Delta\lambda_{eff}$) and branching ratios ($\beta_R$) are obtained and are reported in table 8. The predicted $\beta_R$ values using the JO theory are also presented in table 8.

Decay curves of the luminescence originating from the $^4F_{3/2}$ level of the $Nd^{3+}$ ion in the glasses under investigation have been measured at RT under 355 nm excitation by monitoring the $^4F_{3/2} \rightarrow {}^4I_{9/2}$ emission transition. The decay curves for the PKMAFN glasses at different $Nd^{3+}$ ion concentration are shown in figure 3. All the decay curves show a non-exponential behaviour. From these decay curves, the effective decay times ($\tau_{av}$), which are considered as the experimental lifetime ($\tau_{exp}$) for the $^4F_{3/2}$ level, have been determined by using the following expression [34]:

$$\tau_{exp} = \tau_{av} = \frac{\int t I(t)\,dt}{\int I(t)\,dt} \tag{4}$$

**Table 5.** Wavenumbers ($cm^{-1}$), doubly reduced matrix elements ($\|U^{(\lambda)}\|^2$, $\lambda = 2$, 4 and 6), electric ($f_{ed}$), magnetic ($f_{md}$) and total ($f_{total}$) oscillator strength ($\times 10^{-6}$) for multiplets of the $Nd^{3+}$:PKMAN10 glass.

| S.No. | Multiplet | Wavenumber ($cm^{-1}$) | $\|U^2\|^2$ | $\|U^4\|^2$ | $\|U^6\|^2$ | PKMAN10 | | |
|---|---|---|---|---|---|---|---|---|
| | | | | | | $f_{ed}$ | $f_{md}$ [a] | $f_{total}$ |
| 1 | $^4I_{11/2}$ | 1 771 | 0.019 45 | 0.107 35 | 1.167 03 | 2.293 | 0.205 | 2.498 |
| 2 | $^4I_{13/2}$ | 3 703 | 0.000 09 | 0.013 66 | 0.454 66 | 1.750 | 0 | 1.750 |
| 3 | $^4I_{15/2}$ | 5 725 | 0.000 00 | 0.000 09 | 0.044 59 | 0.259 | 0 | 0.259 |
| 4 | $^4F_{3/2}$ | 11 411 | 0.000 00 | 0.229 98 | 0.057 10 | 2.973 | 0 | 2.973 |
| 5 | $^4F_{5/2}$ | 12 414 | 0.000 53 | 0.231 38 | 0.400 07 | 7.569 | 0 | 7.569 |
| 6 | $^2H(2)_{9/2}$ | 12 678 | 0.008 47 | 0.007 38 | 0.112 96 | 1.632 | 0.016 | 1.648 |
| 7 | $^4F_{7/2}$ | 13 371 | 0.000 92 | 0.042 59 | 0.42 507 | 6.269 | ∼0 | 6.269 |
| 8 | $^4S_{3/2}$ | 13 455 | 0.000 00 | 0.002 16 | 0.233 18 | 3.203 | 0 | 3.203 |
| 9 | $^4F_{9/2}$ | 14 619 | 0.000 91 | 0.009 39 | 0.040 20 | 0.728 | 0.003 | 0.731 |
| 10 | $^2H(2)_{11/2}$ | 15 916 | 0.000 06 | 0.002 63 | 0.009 98 | 0.199 | ∼0 | 0.199 |
| 11 | $^4G_{5/2}$ | 17 217 | 0.898 16 | 0.412 79 | 0.034 03 | 21.122 | 0 | 21.122 |
| 12 | $^2G_{7/2}$ | 17 358 | 0.077 16 | 0.186 72 | 0.034 36 | 4.698 | ∼0 | 4.698 |
| 13 | $^4G_{7/2}$ | 19 092 | 0.053 63 | 0.155 74 | 0.051 53 | 4.564 | ∼0 | 4.564 |
| 14 | $^4G_{9/2}$ | 19 448 | 0.004 72 | 0.060 32 | 0.041 12 | 1.929 | ∼0 | 1.929 |
| 15 | $^2K_{13/2}$ | 19 678 | 0.006 55 | 0.000 22 | 0.029 84 | 0.717 | 0 | 0.717 |
| 16 | $^2G(1)_{9/2}$ | 21 057 | 0.000 99 | 0.015 18 | 0.013 41 | 0.587 | ∼0 | 0.587 |
| 17 | $^2D(1)_{3/2}$ | 21 216 | 0.000 00 | 0.020 17 | 0.000 17 | 0.381 | 0 | 0.381 |
| 18 | $^4G_{11/2}$ | 21 399 | 0.000 01 | 0.005 03 | 0.008 02 | 0.269 | ∼0 | 0.269 |
| 19 | $^2K_{15/2}$ | 21 615 | 0.000 00 | 0.004 43 | 0.013 48 | 0.380 | 0 | 0.380 |
| 20 | $^2P_{1/2}$ | 23 249 | 0.000 00 | 0.036 55 | 0.000 00 | 0.750 | 0 | 0.750 |
| 21 | $^2D(1)_{5/2}$ | 23 874 | 0.000 00 | 0.000 57 | 0.001 35 | 0.045 | 0 | 0.045 |
| 22 | $^2P_{3/2}$ | 26 048 | 0.00000 | 0.00031 | 0.000 45 | 0.019 | 0 | 0.019 |
| 23 | $^4D_{3/2}$ | 28 243 | 0.000 00 | 0.197 83 | 0.017 33 | 5.424 | 0 | 5.424 |
| 24 | $^4D_{5/2}$ | 28 383 | 0.000 09 | 0.056 38 | 0.027 83 | 2.214 | 0 | 2.214 |
| 25 | $^4D_{1/2}$ | 28 720 | 0.000 00 | 0.258 97 | 0.000 00 | 6.561 | 0 | 6.561 |
| 26 | $^2I_{11/2}$ | 29 496 | 0.004 34 | 0.013 48 | 0.003 23 | 0.565 | 0.001 | 0.566 |
| 27 | $^2L_{15/2}$ | 30 209 | 0.000 00 | 0.023 23 | 0.009 46 | 0.908 | 0 | 0.908 |
| 28 | $^4D_{7/2}$ | 30 437 | 0.000 00 | 0.003 73 | 0.008 01 | 0.347 | ∼0 | 0.347 |
| 29 | $^2I_{13/2}$ | 30 852 | 0.000 12 | 0.001 21 | 0.001 64 | 0.087 | 0 | 0.087 |
| 30 | $^2L_{17/2}$ | 31 665 | 0.000 00 | 0.000 92 | 0.001 24 | 0.065 | 0 | 0.065 |
| 31 | $^2H(1)_{9/2}$ | 32 803 | 0.000 12 | 0.007 96 | 0.000 04 | 0.235 | ∼0 | 0.235 |
| 32 | $^2D(2)_{3/2}$ | 33 400 | 0.000 00 | 0.009 60 | 0.000 98 | 0.316 | 0 | 0.316 |
| 33 | $^2H(1)_{11/2}$ | 34 122 | 0.000 14 | 0.000 02 | 0.000 28 | 0.015 | ∼0 | 0.015 |
| 34 | $^2D(2)_{5/2}$ | 34 154 | 0.000 59 | 0.000 81 | 0.003 35 | 0.159 | 0 | 0.159 |
| 35 | $^2F(2)_{5/2}$ | 38 364 | 0.002 21 | 0.003 24 | 0.000 04 | 0.189 | 0 | 0.189 |
| 36 | $^2F(2)_{7/2}$ | 39 735 | 0.000 06 | 0.000 38 | 0.000 70 | 0.044 | ∼0 | 0.044 |
| 37 | $^2G(2)_{9/2}$ | 47 683 | 0.000 05 | 0.001 34 | 0.000 04 | 0.061 | 15.598 | 15.659 |
| 38 | $^2G(2)_{7/2}$ | 48 627 | 0.000 38 | 0.002 17 | 0.000 19 | 0.120 | ∼0 | 0.120 |
| 39 | $^2F(1)_{1/2}$ | 66 420 | 0.000 01 | 0.000 13 | 0.000 50 | 0.042 | 0 | 0.042 |
| 40 | $^2F(1)_{5/2}$ | 67 515 | 0.000 71 | 0.000 96 | 0.000 26 | 0.119 | 0 | 0.119 |

[a] $f_{md}$ is quite negligible (<0.0001) for the transitions $^4F_{7/2}$, $^2H(2)_{11/2}$, $^2G_{7/2}$, $^4G_{7/2}$, $^4G_{9/2}$, $^2G(1)_{9/2}$, $^4G_{11/2}$, $^4D_{7/2}$, $^2H(1)_{9/2}$, $^2H(1)_{11/2}$, $^2F(2)_{7/2}$ and $^2G(2)_{7/2}$.

where $I(t)$ is the emission intensity at time $t$. The obtained $\tau_{exp}$ values are presented in table 9. The quantum efficiency of the $^4F_{3/2}$ level of the $Nd^{3+}$ ion has been evaluated for the present glasses and is also presented in table 9.

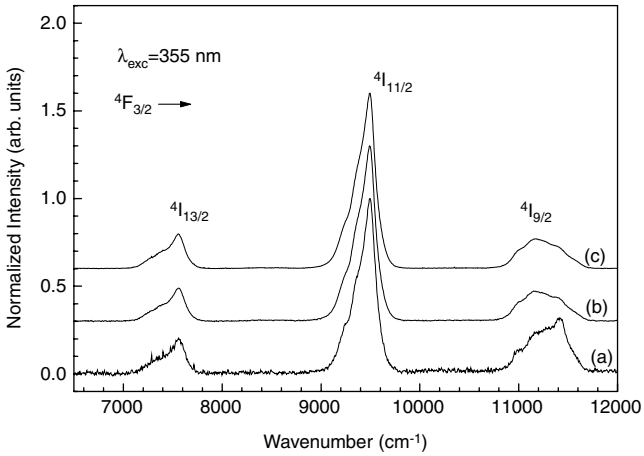


**Figure 2.** Emission spectra of $Nd^{3+}$ ions in (a) PKMAN01, (b) PKMAN10 and (c) PKMAN20 glasses.

**Table 6.** Judd–Ofelt parameters ($\Omega_\lambda \pm 5\%$, $\times 10^{-20}$ $cm^2$), spectroscopic quality factor ($\chi = \Omega_4/\Omega_6$) and radiative lifetime ($\tau_R \pm 2\%$) of the $^4F_{3/2}$ for 1.0 mol% $Nd^{3+}$-doped phosphate glasses and for some of the reported $Nd^{3+}$:glass systems.

| Glass | $\Omega_2$ | $\Omega_4$ | $\Omega_6$ | $\chi$ | $\tau_R$ |
|---|---|---|---|---|---|
| PKMAN10 | 6.22 | 5.95 | 6.83 | 0.871 | 262 |
| PKMAFN10 | 7.66 | 5.15 | 6.99 | 0.737 | 273 |
| PKMABFN10 | 7.34 | 5.97 | 6.69 | 0.892 | 262 |
| Zinc borate [32] | 5.2 | 3.6 | 5.0 | 0.720 | 311 |
| $TeO_2$–LiF–$Nd_2O_3$ [25] | 5.61 | 4.17 | 5.44 | 0.767 | 209 |
| BIGaZLuTMn [30] | 1.26 | 2.58 | 4.08 | 0.632 | 513 |
| 50 $ZnCl_2$–30 $BaCl_2$–20 KCl–1 $NdCl_3$ [29] | 4.97 | 7.39 | 5.12 | 1.443 | — |
| $Bi_2O_3$–PbO–$Ga_2O_3$–$Nd_2O_3$ [27] | 0.95 | 2.01 | 4.30 | 0.467 | 369 |
| 19 ZnO–80 $TeO_2$–1 $Nd_2O_3$ [26] | 4.27 | 4.76 | 4.59 | 1.037 | 130 |
| 58 $P_2O_5$–30 $B_2O_3$–10 $BaF_2$–2 $Nd_2O_3$ [24] | 2.57 | 4.40 | 5.99 | 0.73 | 320 |
| 75 $NaPO_3$–24 $BaF_2$–1 $NdF_3$ [31] | 2.41 | 3.27 | 5.19 | 0.630 | 425 |
| 75 $NaPO_3$–24.5 ZnO–0.5 $Nd_2O_3$ [31] | 3.76 | 3.27 | 5.23 | 0.625 | 410 |
| 35 $Bi_2O_3$–30 $Na_2O$–34 $B_2O_3$–1 $Nd_2O_3$ [16] | 4.72 | 2.12 | 3.93 | 0.54 | 349 |
| 35 PbO–30 $Na_2O$–34 $B_2O_3$–1 $Nd_2O_3$ [16] | 4.81 | 1.97 | 3.94 | 0.50 | 426 |
| $MgF_2$–$BaF_2$–$Al(PO_3)_3$–$Ba(PO_3)_2$–$Nd_2O_3$ [15] | 1.83 | 4.73 | 4.19 | 1.129 | 358 |
| 95 $TeO_2$–4.5 $Nb_2O_5$–0.5 $Nd_2O_3$ [21] | 3.12 | 4.84 | 3.28 | 1.476 | 159 |
| 90 $TeO_2$–9.5 $Nb_2O_5$–0.5 $Nd_2O_3$ [21] | 4.00 | 4.59 | 3.78 | 1.214 | 148 |
| 25 $CdF_2$–13.5 $CdCl_2$–30 NaF–20 $BaF_2$–1.5 $BaCl_2$–10 $ZnF_2$ [28] | 2.81 | 4.62 | 5.22 | 0.885 | 340 |
| ZBLAN [28] | 2.66 | 3.05 | 4.08 | 0.747 | 430 |
| LHG-8 [5] | 4.4 | 5.1 | 5.6 | 0.911 | 351 |
| LG-770 [5] | 4.3 | 5.0 | 5.6 | 0.892 | 349 |
| LHG-80 [5] | 3.6 | 5.0 | 5.5 | 0.909 | 326 |
| LG-750 [5] | 4.6 | 4.8 | 5.6 | 0.857 | 367 |

If the process responsible for the non-exponential decay is cross-relaxation, the decay of luminescence of a donor–acceptor system follows an expression derived by Inokuti and Hirayama (widely known as the IH model) [35]. In the present case the acceptors are the $Nd^{3+}$ ions in the ground state. In the IH model, the emission intensity as a function of time is given

**Table 7.** Emission transitions $|(S, L)J\rangle \rightarrow |(S', L')J'\rangle$, predicted radiative transition probabilities ($A$, $s^{-1}$), branching ratios ($\beta_R$) and lifetimes ($\tau_R$, $\mu s$) of the 1.0 mol% $Nd^{3+}$-doped PKMAN10 glass.

| Initial state | Final state | $A$ ($s^{-1}$) ± 2% | $\beta_R$ ± 2% | $\tau_R$ ($\mu s$) ± 2% |
|---|---|---|---|---|
| $\|(S, L)J\rangle$ | $\|(S', L')J'\rangle$ | | | |
| $^4F_{9/2}$ | $^4S_{3/2}$ | ∼0 | 0 | 249 |
| | $^4F_{7/2}$ | 1 | ∼0 | |
| | $^2H_{9/2}$ | 1 | ∼0 | |
| | $^4F_{5/2}$ | 3 | 0.001 | |
| | $^4F_{3/2}$ | 6 | 0.001 | |
| | $^4I_{15/2}$ | 975 | 0.244 | |
| | $^4I_{13/2}$ | 1424 | 0.356 | |
| | $^4I_{11/2}$ | 1324 | 0.331 | |
| | $^4I_{9/2}$ | 268 | 0.067 | |
| $^4F_{5/2}$ | $^4F_{3/2}$ | ∼0 | ∼0 | 210 |
| | $^4I_{15/2}$ | 170 | 0.036 | |
| | $^4I_{13/2}$ | 941 | 0.198 | |
| | $^4I_{11/2}$ | 569 | 0.120 | |
| | $^4I_{9/2}$ | 3073 | 0.647 | |
| $^4F_{3/2}$ | $^4I_{15/2}$ | 19 | 0.005 | 262 |
| | $^4I_{13/2}$ | 375 | 0.099 | |
| | $^4I_{11/2}$ | 1877 | 0.493 | |
| | $^4I_{9/2}$ | 1538 | 0.404 | |

**Table 8.** Emission peak positions ($\lambda_p$ ± 0.3 nm), effective linewidths ($\Delta\lambda_{eff}$ ± 0.1 nm), experimental and calculated branching ratios ($\beta_R$ ± 2%) and stimulated emission cross-sections ($\sigma(\lambda_p) \pm 0.2 \times 10^{-20}$ $cm^2$) of $^4F_{3/2} \rightarrow$ $^4I_{9/2,11/2,13/2}$ transitions of 1.0 mol % $Nd^{3+}$-doped title glasses.

| | PKMAN10 | | | | | PKMFAN10 | | | | | PKMABFN10 | | | | |
|---|---|---|---|---|---|---|---|---|---|---|---|---|---|---|---|
| | $\lambda_p$ | $\Delta\lambda_{eff}$ | $\beta_R$ | | $\sigma(\lambda_p)$ | $\lambda_p$ | $\Delta\lambda_{eff}$ | $\beta_R$ | | $\sigma(\lambda_p)$ | $\lambda_p$ | $\Delta\lambda_{eff}$ | $\beta_R$ | | $\sigma(\lambda_p)$ |
| Transition $^4F_{3/2} \rightarrow$ | | | Exp | Cal | | | | Exp | Cal | | | | Exp | Cal | |
| $^4I_{13/2}$ | 1322.8 | 40.2 | 0.10 | 0.01 | 1.63 | 1324.5 | 50.2 | 0.13 | 0.10 | 1.34 | 1322.8 | 48.6 | 0.12 | 0.10 | 1.45 |
| $^4I_{11/2}$ | 1053.5 | 28.8 | 0.68 | 0.49 | 4.41 | 1053.7 | 29.5 | 0.64 | 0.51 | 4.40 | 1054.8 | 30.7 | 0.65 | 0.49 | 4.46 |
| $^4I_{9/2}$ | 896.8 | 35.8 | 0.21 | 0.40 | 1.58 | 892.9 | 39.9 | 0.22 | 0.38 | 1.25 | 892.9 | 38.3 | 0.21 | 0.40 | 1.32 |

by

$$I(t) = I_0 \exp\left\{-\frac{t}{\tau_0} - Q\left(\frac{t}{\tau_0}\right)^{3/S}\right\} \tag{5}$$

where $t$ is the time after excitation, and $\tau_0$ is the intrinsic decay time of the donors in the absence of acceptors. $Q$ is the energy transfer parameter defined as

$$Q = \frac{4\pi}{3}\Gamma\left(1 - \frac{3}{S}\right) N_0 R_0^3. \tag{6}$$

$Q$ depends on a number $S$ and the gamma function $\Gamma(x)$, which is equal to 1.77, 1.43 and 1.3 for dipole–dipole ($S = 6$), dipole–quadrupole ($S = 8$) and quadrupole–quadrupole ($S = 10$) interactions, respectively. $N_0$ is the acceptor concentration, which is almost equal to total

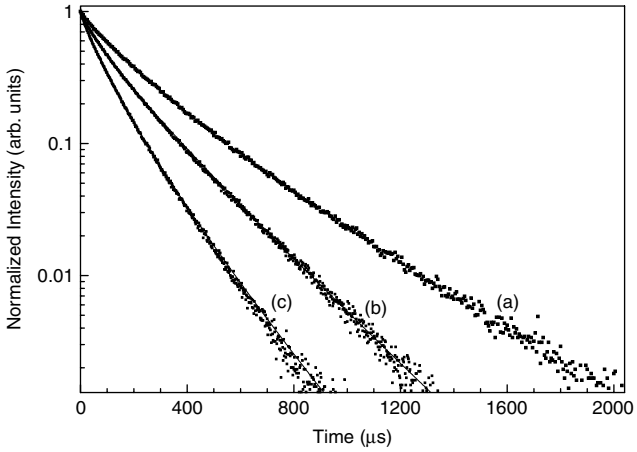


**Figure 3.** Luminescence decay profiles for the $^4F_{3/2} \rightarrow {}^4I_{9/2}$ state of $Nd^{3+}$ ions in (a) PKMAFN01, (b) PKMAFN10 and (c) PKMAFN20 glasses. The scattered points are the experimental data and the solid line is the fit of experimental data to the IH model equation for $S = 6$.

**Table 9.** Experimental lifetimes ($\tau_{exp}$) and quantum efficiencies ($\eta$) of the $^4F_{3/2}$ level, non-radiative transition rates ($W_{NR}$), energy transfer parameters ($Q$), critical distances ($R_0$) and dipole–dipole interaction parameter ($C_{DA}$) for different concentrations (mol%) of $Nd^{3+}$-doped title glasses.

| Glass | $\tau_{exp} \pm 5$ ($\mu$s) | $\eta$ $\pm 0.05$ | $W_{NR} \pm 5$ ($s^{-1}$) | $Q$ $\pm 0.002$ | $R_0$ (Å) $\pm 0.05$ | $C_{DA}$ ($\times 10^{-40}$ $cm^6$ $s^{-1}$) $\pm 0.05$ |
|---|---|---|---|---|---|---|
| PKMAN01 | 226 | 86 | 608 | — | — | — |
| PKMAN10 | 194 | 74 | 1338 | 0.75 | 7.4 | 7.3 |
| PKMAN20 | 135 | 52 | 3591 | 1.20 | 6.8 | 4.4 |
| PKMAFN01 | 263 | 96 | 139 | — | — | — |
| PKMAFN10 | 196 | 72 | 1439 | 0.88 | 7.7 | 7.9 |
| PKMAFN20 | 136 | 50 | 3890 | 2.13 | 7.2 | 5.3 |
| PKMABFN01 | 253 | 96 | 109 | — | — | — |
| PKMABFN10 | 210 | 80 | 945 | 0.70 | 7.3 | 5.7 |
| PKMABFN20 | 153 | 58 | 2719 | 1.20 | 6.8 | 3.7 |

concentration of lanthanide ions, and $R_0$ is the critical distance defined as the donor–acceptor separation for which the rate of energy transfer between a donor and acceptor is equal to the intrinsic decay rate, $\tau_0^{-1}$. The dipole–dipole interaction parameter $C_{DA}$ is related to $R_0$ as

$$C_{DA} = \frac{R_0^{(S)}}{\tau_0}. \tag{7}$$

The decay curves for the present $Nd^{3+}$:glass systems are well fitted to the IH model for $S = 6$, indicating a dipole–dipole interaction between donor and acceptors. The energy transfer parameter ($Q$) has been obtained from the IH model fitting of decay curve, which in turn has been used to calculate the critical distance between the donor and acceptor ($R_0$) using equation (6). The values of $Q$, $R_0$ and $C_{DA}$ are also presented in table 9 for the present $Nd^{3+}$-doped glasses. The important emission characteristics ($\lambda_p$, $\Delta\lambda_{eff}$ and $\sigma(\lambda_p)$) for the $^4F_{3/2} \rightarrow {}^4I_{11/2}$ lasing transition are presented in table 10 and are compared with those of other reported $Nd^{3+}$:glass systems.

**Table 10.** Peak wavelengths ($\lambda_p \pm 0.3$ nm), effective linewidths ($\Delta\lambda_{eff} \pm 0.1$ nm) and stimulated emission cross-sections $\sigma(\lambda_p \pm 0.2\ cm^2)$ for the $^4F_{3/2} \rightarrow {}^4I_{11/2}$ laser transition of $Nd^{3+}$:glass systems.

| Glass | $\lambda_p$ | $\Delta\lambda_{eff}$ | $\sigma(\lambda_p)$ |
|---|---|---|---|
| PKMAN10 | 1053.5 | 28.8 | 4.41 |
| PKMAFN10 | 1053.7 | 29.5 | 4.40 |
| PKMABFN10 | 1054.8 | 30.7 | 4.46 |
| Zinc borate [32] | 1060 | 37.9 | 2.64 |
| $TeO_2$–LiF–$Nd_2O_3$ [25] | 1062 | 30.2 | 4.27 |
| $Bi_2O_3$–PbO–$Ga_2O_3$–$Nd_2O_3$ [27] | 1066 | — | 1.1 |
| 95 $TeO_2$–4.5 $Nb_2O_5$–0.5 $Nd_2O_3$ [21] | 1062 | 32.9 | 3.38 |
| 90 $TeO_2$–9.5 $Nb_2O_5$–0.5 $Nd_2O_3$ [21] | 1062 | 30.8 | 3.97 |
| 35 $Bi_2O_3$–30 $Na_2O$–34 $B_2O_3$–1 $Nd_2O_3$ [16] | 1067 | 43 | 2.0 |
| 35 PbO–30 $Na_2O$–34 $B_2O_3$–1 $Nd_2O_3$ [16] | 1065 | 43 | 1.8 |
| $MgF_2$–$BaF_2$–$Al(PO_3)_3$–$Ba(PO_3)_2$–$Nd_2O_3$ [15] | 1058 | 32 | 2.68 |
| CSPN [19] | 1062 | 36.4 | 2.5 |
| PKBN [18] | 1059 | 29.3 | 2.78 |
| LHG-8 [15] | 1053 | 26.5 | 3.6 |
| LG-770 [5] | 1053 | 25.4 | 3.9 |
| LHG-80 [5] | 1054 | 23.9 | 4.2 |
| LG-750 [5] | 1053.5 | 25.3 | 3.7 |

## 5. Discussion

The spectroscopic properties such as absorption and emission cross-sections, peak wavelengths and linewidths, lifetimes and quantum efficiencies and emission quenching due to ion–ion interactions of the lanthanide ions are dependent upon the chemical composition of the host glass. Fluorescence quenching in highly concentrated neodymium materials is a problem of practical as well as theoretical importance. The $Nd^{3+}$ concentration has to be kept within an optimum range to obtain maximum laser output. For maximum coupling to flash lamp pumping, a material with a long fluorescence lifetime and high absorption cross-section is desirable. However, high absorption cross-section requires high $Nd^{3+}$ ion concentration, but this reduces the fluorescence lifetime of the excited states, so the $Nd^{3+}$ ion concentration should be optimized to have maximum absorption and fluorescence lifetime [1]. The results of the most recent review report on $Nd^{3+}$-doped phosphate laser glasses [5] suggest that the optimum active ion concentration for obtaining efficient laser emission should be around 1.0 mol% of $Nd^{3+}$ ions.

### *5.1. Energy level analysis*

Energy level analysis has been carried out by an f-shell empirical program [36]. The energy values for various levels of $Nd^{3+}$ ions in PKMAN10, PKMAFN10 and PKMABFN10 glasses, which are obtained from their respective absorption and emission spectra (table 2), are used for the energy level analysis. The initial free-ion values are taken from those given by Jayasankar *et al* [37] for $Nd^{3+}$:$LaCl_3$. Among the various interactions that contribute to the total free-ion Hamiltonian, the major contribution comes from the inter-electronic ($F^k$) and the spin–orbit ($\zeta$) interactions which govern the $^{2S+1}L_J$ level positions. The rest of the terms will only give corrections to the energy of these levels without removing their degeneracy. Hence, during the fitting process, after observing the trends and consistency, out of 20 free-ion parameters, the only parameters that were allowed to vary were $F^k$ and $\zeta$, to have a systematic comparison.

During the fitting process, the four atomic parameters $M^2$, $M^4$, $P^4$ and $P^6$ were constrained according to $M^2 = 0.56M^0$, $M^4 = 0.38M^0$, $P^4 = 0.75P^2$ and $P^6 = 0.50P^2$ and the values of $\alpha = 22.12$, $\beta = -656$, $\gamma = 1583$, $T^2 = 372$, $T^3 = 40$, $T^4 = 61$, $T^6 = -291$, $T^7 = 347$, $T^8 = 355$, $M^0 = 1.84$ and $P^2 = 281$ were fixed to the values of $Nd^{3+}$:$LaCl_3$ [37]. Table 3 presents the best-fit free-ion parameters ($F^k$ and $\zeta$) obtained for the present systems along with those calculated for other $Nd^{3+}$:glass systems. Using these parameters the calculated energy levels are obtained by diagonalizing the energy matrix of $4f^3$ ($Nd^{3+}$) configuration and they are presented for the present glasses in table 2.

The sum of the Slater parameters, $\Sigma F^k$, which indicates the net electrostatic interaction experienced by $Nd^{3+}$ ions in the host matrix, is also presented in table 3. $\Sigma F^k$ follows the trend CSPN < ZBN < BIGZLTM < TLN < NCN < PKMABFN10 < PKMAFN10 < PKMAN10 < PKBN. From the trend of $\Sigma F^k$, it is clear that $Nd^{3+}$ ions are experiencing relatively more electrostatic force in phosphate-based glasses than in other glass hosts. The trend of the magnitude of $\Sigma F^k$ also suggests that though there is a decrease in the net electrostatic effect experienced by the $Nd^{3+}$ ion with addition of the fluorine content to the pure phosphate glass, it is very much less. However, the hydrogenic ratios, $F^2/F^4$ (∼1.35), and $F^2/F^6$ (∼2.05), are more or less similar for all the present as well as for other reported $Nd^{3+}$:glass systems that are presented in table 3. This indicates that the radial integral part of the f-orbital of the $Nd^{3+}$ ions remains unchanged even though the glass compositions are changed from glass to glass, which is mainly due to shielding of 4f electrons by the $5s^2$ and $5p^6$ orbitals.

### *5.2. Judd–Ofelt analysis and radiative lifetimes*

The absorption spectra of 1.0 mol% $Nd^{3+}$-doped PKMAN10, PKMAFN10 and PKMABFN10 glasses consists of a group of inhomogeneously broadened absorption bands characteristic for the $4f^3$–$4f^3$ transition of trivalent neodymium, which are located in the ultraviolet, visible and the infrared regions. Among various absorption transitions of the $Nd^{3+}$ ion, the absorption band assigned to the $^4I_{9/2} \rightarrow {}^4G_{5/2}$ transition centred at around 580 nm is referred to as a hypersensitive transition since it follows the selection rule $|\Delta S| = 0$, $|\Delta L| \leqslant 2$ and $|\Delta J| \leqslant 2$. It is also well known that the $^4I_{9/2} \rightarrow {}^4G_{5/2}$ transition of the $Nd^{3+}$ ion overlaps with the $^4I_{9/2} \rightarrow {}^2G_{7/2}$ transition. The intensity of this hypersensitive transition strongly depends on the ion–ligand bonding environment. From table 4, it can be noted that the total oscillator strength of the $^4I_{9/2} \rightarrow {}^4G_{5/2} + {}^2G_{7/2}$ transitions is much higher than those of the other transitions for the present glass systems as well as for other reported $Nd^{3+}$-doped glass systems except for the $TeO_2$-based glass systems. From figure 1, it is clear that some of the absorption bands are overlapping with each other and in those cases the matrix elements, $\langle \|U^{(\lambda)}\| \rangle^2$, of the corresponding transitions were summed while calculating the JO parameters. Table 5 clearly shows that the magnetic dipole contribution to the total oscillator strength is negligible for the absorption transitions of $Nd^{3+}$ ions in the PKBAN10 glass. Also it is worth noting that the magnetic dipole oscillator strengths are host independent. As the ratio between the magnetic dipole to electric dipole oscillator strength is quite negligible, all the absorption transitions are assumed as induced electric dipole allowed and magnetic dipole contributions were not taken into account for calculating the phenomenological JO parameters.

The magnitudes of the JO parameters for PKMAN10, PKMAFN10 and PKMABFN10 glasses are found to be relatively higher than those of the other reported glass systems, including the commercial laser glasses LHG-80, LHG-8, LG-770 and LG-750 [5]. The JO parameter $\Omega_2$ indicates the covalence of the metal–ligand bond, whereas $\Omega_4$ and $\Omega_6$ indicate the rigidity of the host matrix [38]. The larger value of $\Omega_2$ is due to the relatively higher value of the oscillator

strength of the hypersensitive transition. The larger value of the $\Omega_2$ for the present studied systems indicates a strong covalence of the metal–ligand bond [38]. When the pure phosphate glasses are modified with fluorine content, the strength of this covalent bond increases and further, $AlF_3$ is found to have notable influence on the metal–ligand bond covalence. To give an idea of the nature of the $Nd^{3+}$–ligand bond, nephelauxetic ratios and bonding parameters have also been evaluated. The nephelauxetic ratio ($\beta$) is given by [7–9]

$$\beta = \frac{\bar{\nu}_c}{\bar{\nu}_a} \tag{8}$$

where $\bar{\nu}_c$ is the wavenumber (in $cm^{-1}$) of a particular transition for an ion in the host under investigation and $\bar{\nu}_a$ is the wavenumber (in $cm^{-1}$) of the same transition for the aquo ion. From the average values of $\beta$ (taken as $\bar{\beta}$), the bonding parameter, $\delta$, can be calculated by an expression [7–9]

$$\delta = \frac{1 - \bar{\beta}}{\bar{\beta}}. \tag{9}$$

The metal–ligand bond will be covalent or ionic depending upon the positive or negative sign of $\delta$. Since the sign of $\delta$ is negative (shown in table 1(b)), the $Nd^{3+}$–ligand bond in the glass systems of the present investigation is of ionic type. Moreover, this ionic nature is found to increase with the addition of $AlF_3$ and decrease with the addition of $BaF_2$ to the phosphate glass host. This seems to be contrary to the results obtained from the Judd–Ofelt analysis; however, we note that also the asymmetry of the sites accommodating the $Nd^{3+}$ ions contributes to the values of the $\Omega_2$ JO parameter, as this value increases with the site distortion [39]. It is conceivable that asymmetry and covalency give different contributions in the different glass hosts and that the degree of asymmetry is increased by the introduction of fluoride ions in the lanthanide coordination sphere.

It is well known that the luminescence from the excited $^4F_{3/2}$ level to the $^4I_J$ ($J = 9/2, 11/2, 13/2$ and $15/2$) manifolds depends only on the $\Omega_4$ and $\Omega_6$ parameters, since the matrix elements, $\langle {}^4F_{3/2} \| U^{(2)} \| {}^4I_J \rangle^2$, are equal to zero. Hence, $\beta_R$ values for transitions from the $^4F_{3/2}$ level are a function of the ratio $\Omega_4/\Omega_6$, which is widely known as the spectroscopic quality factor ($\chi$), and do not depend on the parameters $\Omega_4$ and $\Omega_6$ separately [40]. On increasing the value of $\chi$, the branching ratio of the $^4F_{3/2} \rightarrow {}^4I_{9/2}$ transition increases while that of the $^4F_{3/2} \rightarrow {}^4I_{11/2}$ one decreases. Hence, to maximize the emission intensity of the $^4F_{3/2} \rightarrow {}^4I_{11/2}$ transition it is preferable to have $\Omega_4 \ll \Omega_6$ and therefore the $\chi$ value should be as small as possible. The $\chi$ values of the present glasses are comparable to those of commercial laser glasses, LHG-80, LHG-8, LG-770 and LG-750. Further, when pure phosphate glass is modified with $AlF_3$, the $\chi$ value becomes smaller but there is a slight increase in the $\chi$ value when the phosphate glass is modified with $BaF_2$. From table 6, it is clear that PbO- and/or $Bi_2O_3$-based glasses have lower $\chi$ values. The JO parameters can be used to predict $\tau_R$ of the $^4F_{3/2}$ level of the $Nd^{3+}$ ion. The radiative lifetimes of the $^4F_{3/2}$ level for the glasses under investigation are also presented in table 6 along with those reported for other $Nd^{3+}$:glasses. The $\tau_R$ values are found to be comparable with those of other $Nd^{3+}$:glasses but are lower than those of commercial glasses. As can be seen from table 6, it is clear that $TeO_2$-based glass systems possess shorter lifetimes whereas multicomponent fluoride glass systems possess longer lifetimes.

### *5.3. Emission properties*

From the $^4F_{3/2} \rightarrow {}^4I_J$ emission spectra of the glasses under investigation (see figure 2), the radiative properties have been calculated and are presented in table 8. From table 8, it can be

noted that fluorine content has a negligible effect on the emission properties. As can be seen from table 10, the peak wavelength of the $^4F_{3/2} \rightarrow {}^4I_{11/2}$ transition for the title glasses is almost similar to those of commercial glasses whereas the $\Delta\lambda_{eff}$ value is found to be higher for the title glasses than the commercial glasses. The peak stimulated emission cross-sections of the title glasses are found to be higher than those of all the glass hosts, including the commercial glasses (see table 10).

### *5.4. Fluorescence lifetime and non-radiative properties*

The emission decay curves of the present glasses are found to be non-exponential even for the glass with lower concentration of the $Nd^{3+}$ ion (0.1 mol%). Figure 3 shows the decay profiles of the PKMAFN glasses which are almost similar to those of PKMAN and PKMABFN glass systems and are not shown in the figure. This kind of non-exponential behaviour of the decay curves with low $Nd^{3+}$ ion concentration was also reported in the literature for phosphate [1, 18] and fluorophosphate [7, 15] glasses.

Among the non-radiative processes, the cross-relaxation rate and energy transfer to impurities can be minimized if one controls the active ion concentration and the glass composition. It is well known that the effective phonon energy of a typical phosphate glass lies between 1200 and 1350 $cm^{-1}$ [25, 41, 42], and for the present glass hosts the energy difference between the luminescent $^4F_{3/2}$ level and the next lower $^4I_{15/2}$ level is around 5650 $cm^{-1}$ (from the energy values reported in table 2). Hence, four to five phonons are enough to bridge this energy gap, leading to considerable multiphonon relaxation of the fluorescent $^4F_{3/2}$ level. If only the multiphonon relaxation is considered for the non-radiative processes, then we can write

$$W_{NR} = W_{MP} = \frac{1}{\tau_{exp}} - \frac{1}{\tau_R}. \tag{10}$$

The values of $W_{NR}$ for various concentrations of $Nd^{3+}$ ions in the title glasses are given in table 9. These non-radiative rates are comparable with those reported for $Nd^{3+}$-doped phosphate and silicate glasses [43].

An important non-radiative channel of de-excitation of the excited levels is the cross-relaxation process between the active $Nd^{3+}$ ions, which can be responsible for the non-exponential behaviour of the decay curves in the present glasses. The proposed cross-relaxation process can be represented by $(^4F_{3/2}, {}^4I_{9/2}) \rightarrow (^4I_{15/2}, {}^4I_{15/2})$ [7], as there is a good energy matching (around 5700 $cm^{-1}$) between these levels [7]. In order to estimate the ion–ion interaction, the IH model [35] has been applied to the decay profiles. The values of $Q$, $R_0$ and $C_{DA}$ parameters are presented in table 9. From table 9, it is clear that the magnitude of $Q$ is increasing and critical distance between the donor (excited $Nd^{3+}$) and acceptor (non-excited $Nd^{3+}$) decreases on increasing the $Nd^{3+}$ ion concentration, which clearly indicates enhancement of energy transfer process between $Nd^{3+}$ ions through cross-relaxation. The $R_0$ values obtained for commercial glasses are 6.38, 6.52 and 4.1 Å for LG-770, LHG-8 [44] and LG-750 [45], respectively. The $R_0$ values of the present glass systems are slightly higher than these values. On the other hand PKBN glass [18] has an $R_0$ value equal to 8.4 Å, which is slightly higher than the title glasses. For pure multicomponent fluoride glass, the $R_0$ and $C_{DA}$ values are 6.9 Å and $2.5 \times 10^{-40}$ $cm^6$ $s^{-1}$, respectively [46]. Lupei *et al* [47] determined the $C_{DA}$ value for Nd:YAG to be $1.8 \times 10^{-40}$ $cm^6$ $s^{-1}$ and for the $Nd^{3+}$:$YAlO_3$ [48] system the $C_{DA}$ value was found to be $1.5 \times 10^{-40}$ $cm^6$ $s^{-1}$. $C_{DA}$ values obtained for the present glass systems are slightly higher in magnitude compared to these values.

## 6. Conclusions

In the present investigation, optical properties of $Nd^{3+}$ ions in phosphate-based glasses modified with $BaF_2$ and $AlF_3$ have been determined and are compared with those reported for other $Nd^{3+}$:glass hosts. The electronic structure of the $Nd^{3+}$ ions in these glasses has been deduced from the optical absorption and emission spectra through a free-ion Hamiltonian model. From the absorption spectra, oscillator strengths of various absorption bands are evaluated. The oscillator strengths of the hypersensitive $^4I_{9/2} \rightarrow {}^4G_{5/2} + {}^2G_{7/2}$ transitions in the present glass systems are found to be higher than those of reported $Nd^{3+}$-doped glasses, resulting in a higher value of the Judd–Ofelt parameter, $\Omega_2$. For the luminescent $^4F_{3/2} \rightarrow {}^4I_{11/2}$ transition, the peak position occurs at 1053.5 nm, which is similar to that in commercial LG-750 glass. The lasing properties such as peak wavelengths, effective fluorescence bandwidths and emission cross-sections are found to be higher for the present glasses than those of commercial laser glasses, but the radiative lifetimes are found to be less than those of commercial glasses. The non-radiative decay rates and the critical distances between the donors and acceptors in the present $Nd^{3+}$:glass systems are found to be comparable with those of other reported $Nd^{3+}$:glass systems.

## Acknowledgments

One of the authors (CKJ) is grateful to DAE-BRNS, Government of India, for the sanction of major research project (sanction No. 2003/34/4-BRNS/600, dated 11-07-2003). Part of this work has been carried out under MIUR of Italy.

## References

[1] Brown D C 1981 *High-Peak-Power Nd: Glass Laser Systems* (*Springer Series in Optical Sciences*) (Berlin: Springer)
[2] Ehrmann P R, Carlson K, Campbell J H, Click C A and Brow R K 2004 *J. Non-Cryst. Solids* **349** 105
[3] Kirkpatrick R J and Brow R K 1995 *Solid State Nucl. Magn. Reson.* **5** 9
[4] Poirier G, Cassanjes F C, de Araujo C B, Jerez V A, Ribeiro S L J, Messaddeq Y and Poulain M 2003 *J. Appl. Phys.* **93** 3259
[5] Campbell J H and Suratwala T I 2000 *J. Non-Cryst. Solids* **263/264** 318
[6] Jiang S, Luo T, Myers M, Myers J, Lucas J and Peyghambarian N 1998 *Proc. SPIE* **3280** 2
[7] Balakrishnaiah R, Babu P, Jayasankar C K, Joshi A S, Speghini A and Bettinelli M 2006 *J. Phys.: Condens. Matter* **18** 165
[8] Jayasankar C K and Ravi Kanth Kumar V V 1996 *Physica* B **226** 313
[9] Renuka Devi A and Jayasankar C K 1995 *Mater. Chem. Phys.* **42** 106
[10] Judd B R 1962 *Phys. Rev.* **127** 750
[11] Ofelt G S 1962 *J. Chem. Phys.* **37** 511
[12] Carnall W T 1979 *Handbook on the Physics and Chemistry of Rare-Earths* vol 3, ed K A Gschneidner Jr and L R Eyring (Amsterdam: Elsevier) chapter 24
[13] Görller-Walrand C and Binnemans K 1998 *Handbook on the Physics and Chemistry of Rare-Earths* vol 25, ed K A Gschneidner Jr and L Eyring (Amsterdam: Elsevier) chapter 167
[14] Carnall W T, Fields P R and Rajnak K 1968 *J. Chem. Phys.* **49** 4424
[15] Choi J H, Margaryan A, Margaryan A and Shi F G 2005 *J. Lumin.* **111** 167
[16] Karthikeyan B, Philip R and Mohan S 2005 *Opt. Commun.* **246** 153
[17] Zhao Q Z, Qiu J R, Jiang X W, Zhou Q L, Zhao C J and Zhu C S 2005 *Opt. Mater.* **27** 1159
[18] Ajroud M, Haouari M, Ben Ouada H, Maaref H, Brenier A and Garapon C 2000 *J. Phys.: Condens. Matter* **12** 3181
[19] Pardo J A, Pena J I, Merino R I, Cases R, Larrea A and Orera V M 2002 *J. Non-Cryst. Solids* **298** 23
[20] Courrol L C, De Lima B L S, Kassab L R P, Cacho V D D, Tatumi S H, Gomes L and Wetter N U 2004 *J. Non-Cryst. Solids* **348** 98

[21] Zambelli M, Speghini A, Ingletto G, Locatelli C, Bettinelli M, Vetrone F, Boyer J C and Capobianco J A 2004 *Opt. Mater.* **25** 215
[22] Falcao-Filho E L, de Araujo C B and Messaddeq Y 2002 *J. Appl. Phys.* **92** 3065
[23] Menezes L de S, Maciel G S, de Araujo C B and Messaddeq Y 2001 *J. Appl. Phys.* **90** 4498
[24] De la Rosa-Cruz E, Kumar G A, Diaz-Torres L A, Martinez A and Barbosa-Garcia O 2001 *Opt. Mater.* **18** 321
[25] Ravi Kanth Kumar V V, Bhatnagar A K and Jagannathan R 2001 *J. Phys. D: Appl. Phys.* **34** 1563
[26] Rolli R, Gatterer K, Wachtler M, Bettinelli M, Speghini A and Ajo D 2001 *Spectrochim. Acta* A **57** 2009
[27] Kassab L R P, Tatumi S H, Mendes C M S, Courrol L C and Wetter N U 2000 *Opt. Express* **6** 104
[28] Fernandez J, Balda R and Adam J L 1998 *J. Phys.: Condens. Matter* **10** 4985
[29] Shojiya M, Takahashi M, Kanno R, Kawamoto Y and Kadono K 1998 *Appl. Phys. Lett.* **72** 882
[30] Azkargorta J, Iparraguirre I, Balda R, Fernandez J, Denoue E and Adam J L 1994 *J. Quantum Electron.* **30** 1862
[31] Binnemans K, Van Deun R, Görller-Walrand C and Adam J L 1998 *J. Alloys Compounds* **275–277** 455
[32] Pozza G, Ajo D, Bettinelli M, Speghini A and Casarin M 1996 *Solid State Commun.* **97** 521
[33] Carnall W T, Fields P R and Wybourne B G 1965 *J. Chem. Phys.* **42** 3797
[34] Nakazawa E 1999 *Phosphor Handbook* ed S Shionoya and W M Yen (Boca Raton, FL: CRC Press) p 104
[35] Inokuti M and Hirayama F 1965 *J. Chem. Phys.* **43** 1978
[36] Reid M F, private communication, University of Canterbury, New Zealand
[37] Jayasankar C K, Richardson F S and Reid M F 1989 *J. Less-Common Met.* **148** 286
[38] Jorgensen C K and Reisfeld R 1983 *J. Less-Common Met.* **93** 107
[39] Reisfeld R 1975 *Struct. Bonding* **22** 123
[40] Kaminskii A A and Li L 1974 *Phys. Status Solidi* a **26** K21
[41] Haouari M, Ben Quada H, Maaref H, Hommel H and Legrand A P 1997 *J. Phys.: Condens. Matter* **9** 6711
[42] Babu P, Seo H J, Jang K H, Balakrishnaiah R, Jayasankar C K and Joshi A S 2005 *J. Phys.: Condens. Matter* **17** 4859
[43] Toratani H, Izumitani T and Kuroda H 1982 *J. Non-Cryst. Solids* **52** 303
[44] Ehrmann P R and Campbell J H 2002 *J. Am. Ceram. Soc.* **85** 1061
[45] Fujimoto Y and Nakatsuka M 1997 *J. Non-Cryst. Solids* **215** 182
[46] de Sousa D F, Batalioto F, Bell M J V, Oliveira S L and Nunes L A O 2001 *J. Appl. Phys.* **90** 3308
[47] Lupei V, Lupei A, Georgescu S and Yen W M 1989 *J. Appl. Phys.* **66** 3792
[48] Lupei V, Lupei A and Georgescu S 1992 *J. Phys.: Condens. Matter* **4** L221